Mass-Spectrometric Differentiation of Di*exo*- and Di*endo*-Fused Isomers of Norbornane/ene-Condensed 2-Thiouracil and 1,3-Thiazino[3,2-*a*]-Pyrimidine Derivatives: Stereoselectivity of Retro-Diels-Alder Fragmentations Under EI and CI Conditions

Vladimir V. Ovcharenko, Rousten A. Shaikhutdinov,* and Kalevi Pihlaja
Department of Chemistry, University of Turku, Turku, Finland

Géza Stájer
Institute of Pharmaceutical Chemistry, University of Szeged, Szeged, Hungary

The stereoisomers of the title compounds produce nearly identical electron ionization (EI) mass spectra, which are dominated in the case of the norbornene-condensed derivatives by retro-Diels-Alder (RDA) fragmentation of the hydrocarbon ring. The RDA fragmentation mainly occurs with H transfer and gives rise to $[M–C_5H_5]^+$. For the norbornane-condensed derivatives, the main fragmentation routes include the formation of $[M–C_5H_7]^+$ (protonated thiouracil) and $[M–C_7H_9]^+$ (only from thiazinopyrimidines). The latter species are formed via RDA decomposition of the pyrimidone subunit of the heterocyclic system, a process previously observed for cyclohexane-condensed analogs of these compounds. Only minor differences could be detected between the EI spectra of the di*exo* and di*endo* isomers. Under chemical ionization (CI) conditions, the norbornane-condensed compounds produced no significant fragment peaks with either isobutane or methane as reagent gas. In contrast, the isobutane and methane CI spectra of the norbornene-condensed compounds exhibited prominent peaks of $[MH–C_5H_6]^+$ and $[(M+C_xH_y)–C_5H_6]^+$ originating from moderately stereoselective RDA fragmentations. The relative abundances of the RDA ions obtained from the respective stereoisomers with the same reagent gas were consistently different over a range of experimental conditions. The non-occurrence of RDA fragmentation of the thiazinopyrimidine ring under CI conditions suggested that its energy of activation is higher than that for either of the norbornene-ring RDA fragmentations (with or without H transfer) observed under EI and CI conditions. (J Am Soc Mass Spectrom 2001, 12, 1011–1019) © 2001 American Society for Mass Spectrometry

Various RDA fragmentations are quite common in organic mass spectrometry. The stereochemical implications of mass-spectrometric RDA fragmentations under EI and CI conditions have been thoroughly reviewed in [1]. In addition to these classical techniques, RDA fragmentations have been reported to occur under soft ionization conditions. Some recent examples which demonstrate the universal nature of RDA fragmentations in organic mass spectrometry include such pharmacologically important substances as green tea catechins (FAB) [2a], anti-HIV dideoxycytidine (negative-ion ESI) [2b], and plant flavanols (positive- and negative-ion APCI) [2c].

Stereospecificity is an important aspect of mass-spectrometric RDA fragmentations. In fused polycyclic molecules, it may be manifested either by the predominant RDA fragmentation of *cis*-fused isomers compared with their *trans*-fused counterparts or by the specific stereochemical configuration retained in the fragment ions that originate from different stereoisomers. High stereospecificity of a given RDA fragmentation is indicative of a single-step, concerted reaction mechanism [3].

Previously, we have observed highly stereospecific RDA fragmentations of *cis* and *trans* cyclohexene-fused polycyclic N,O-heterocycles under EI [4] and electro-

Published online July 18, 2001

Address reprint requests to Dr. K. Pihlaja, Department of Chemistry, University of Turku, FIN-20014, Finland. E-mail: kpihlaja@utu.fi

*Permanent address: Department of Chemistry, Kazan State University, Kazan, 420 008 Tatarstan, Russian Federation.

1044-0305/01/$20.00
PII S1044-0305(01)00280-X

Received January 8, 2001
Revised May 3, 2001
Accepted May 7, 2001

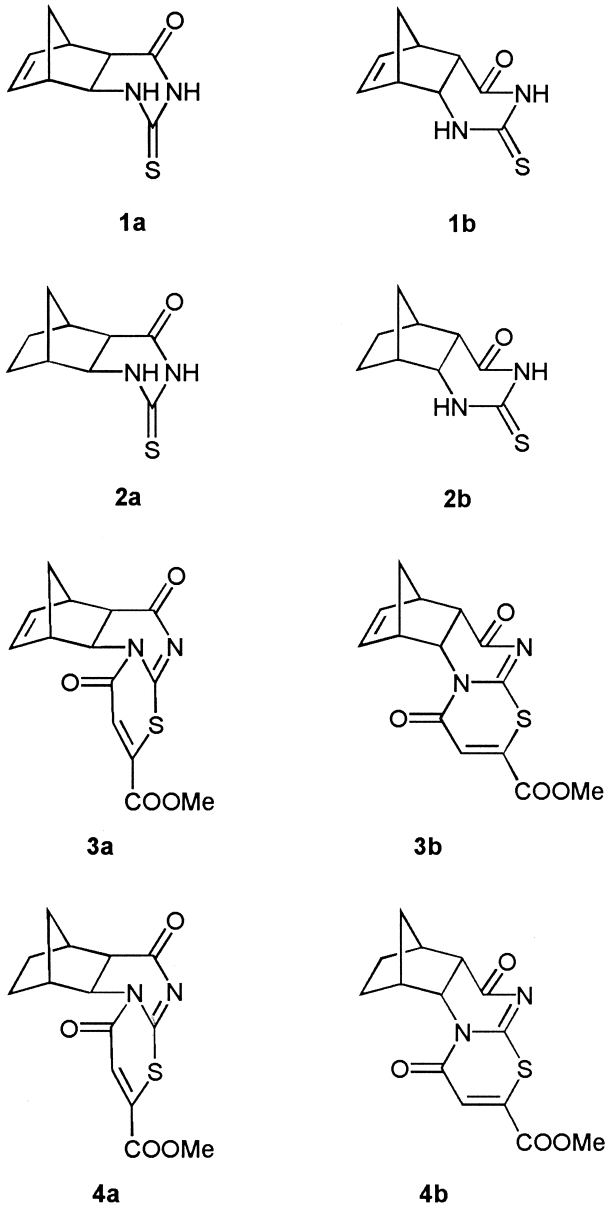

Scheme 1. Structures of compounds **1–4**.

spray (ESI) [5] conditions. However, the di*exo* and di*endo* norbornene-fused analogs of these compounds only exhibited non-stereospecific RDA fragmentations under EI. In a continuation of our studies on cycloalkane/cycloalkene-condensed 2-thiouracil derivatives [6], isomeric norbornane- and norbornene-fused compounds (Scheme **1**) were synthesized. The stereochemically assigned structures were proven by NMR spectroscopy [7].

Experimental

The low-resolution EI mass spectra were obtained by using a VG ZabSpec mass spectrometer (Manchester, UK) at 70 eV (direct insertion probe, ion source temperature 160 °C). Elemental compositions of fragment ions were determined within an average accuracy of 0.5 ppm based on accurate mass measurements at a resolution of 10,000–12,000 (10% valley definition) by the peak matching technique, using perfluorokerosene (PFK) as a reference compound. Metastable ion spectra (B/E and B^2/E are linked scans in which the magnetic field strength, B, and the electrostatic sector voltage, E, are maintained in a fixed relationship, decompositions occurred in the first field free region) were recorded with the same instrument. All the fragmentation processes shown in the schemes were observed in the metastable ion spectra.

CI spectra were recorded on the same instrument under the following operating conditions: CI inner source temperature, 150 °C; ionization energy, 45 eV; emission current, 0.2 mA. Isobutane and methane (AGA Special Gas, Sweden; 99.95% purity) were used as reagent gases. The gas purity proved to be satisfactory, as there were only the usual background ions (*m/e* 43 and 57 for isobutane, *m/e* 17, 29, and 41 for methane; no peaks of H_3O^+ or NH_4^+). The reagent gas pressure in the inner source was maintained at (2–3) $\times$ 10^{-5} mbar. Samples were introduced with a direct insertion probe, which was heated to 140–200 °C in the case of **3**. Spectra of stereoisomers were always recorded on the same date at the same reagent gas pressure.

Results and Discussion

EI Spectra

The 70-eV EI mass spectra of compounds **1–4** (Scheme **1**) listed in Table 1 reveal only a few differences between the spectra of each pair of stereoisomers. The molecular ions are predictably more stable in the case of norbornane-fused **2** and **4** compared with their norbornene-fused analogs (Table 2). Among the norbornene-fused compounds, the thiouracil derivatives **1** form more stable molecular ions (7–8% TIC) than their thiazinopyrimidine counterparts **3**.

The RDA fragmentations in norbornene-fused **1** and **3** produce abundant $[M–C_5H_5]^+$ and $C_5H_6^{+\cdot}$ ions. Apart from this carbocyclic RDA fragmentation to form cyclopentadiene, there are also observed heterocyclic RDA fragmentations in the thiazinopyrimidine derivatives **3** and **4**, which produce either $C_7H_8^{+\cdot}$ or $[M–C_7H_9]^+$ (Table 2). Abundant $C_5H_6^{+\cdot}$ is also formed from the norbornane-fused thiazinopyrimidine derivatives **4** (but not from **2**). Although they seem to originate partly from $M^{+\cdot}$ and $[M–CO]^{+\cdot}$ by a process other than RDA, $C_7H_{10}^{+\cdot}$ and $C_7H_9^+$ (resulting from the RDA decomposition of the pyrimidone ring) are the main precursors of $C_5H_6^{+\cdot}$ (as seen from metastable transitions) in the case of **4**. This explains the much lower abundance of $C_5H_6^{+\cdot}$ in the spectra of norbornane-fused thiouracils **2**, where neither carbocyclic nor heterocyclic RDA fragmentation is possible. The $[M–C_5H_5]^+$ formed from the norbornene-fused compounds via carbocyclic RDA fragmentation accompanied by H transfer is further

Table 1. 70-eV EI mass spectra showing peaks of >5% relative abundance (RA) for **1–4**

Compound	*m/z* (% RA)
1a,**b**	di*exo* **1a**: 194(M, 27) 131(5) 130(7) 129(88) 128(29) 77(6) 70(30) 69(17) 67(7) 66(100) 65(13) 42(6) 40(7) 39(13)
	di*endo* **1b**: 194(M, 31) 131(5) 130(7) 129(86) 128(29) 77(5) 70(29) 69(17) 67(7) 66(100) 65(12) 42(6) 40(8) 39(14)
2a,**b**	di*exo* **2a**: 198(6) 197(13) 196(M, 100) 131(8) 130(55) 129(55) 128(12) 112(5) 102(6) 81(5) 80(6) 77(5) 70(15) 69(8) 68(6) 67(20) 66(14) 65(6) 53(8) 42(5) 41(13) 39(12)
	di*endo* **2b**: 198(6) 197(13) 196(M, 100) 131(9) 130(39) 129(72) 128(15) 112(6) 102(4) 81(6) 80(7) 77(7) 70(17) 69(9) 68(7) 67(18) 66(11) 65(6) 53(8) 42(6) 41(13) 39(12)
3a,**b**	di*exo* **3a**: 304(M, <0.5) 241(8) 240(13) 239(100) 207(9) 95(5) 92(15) 91(35) 85(8) 66(60) 65(10) 39(6)
	di*endo* **3b**: 304(M, <0.5) 241(8) 240(14) 239(100) 207(11) 95(5) 92(5) 91(20) 85(8) 66(58) 65(10) 39(6)
4a,**b**	di*exo* **4a**: 307(6) 306(M, 33) 278(32) 214(7) 213(65) 212(8) 211(10) 94(8) 93(6) 91(5) 85(11) 79(7) 77(8) 67(10) 66(100) 65(7) 53(7) 41(6) 39(7)
	di*endo* **4b**: 307(7) 306(M, 37) 278(23) 214(6) 213(56) 212(9) 211(12) 94(7) 93(7) 91(5) 85(9) 79(8) 77(8) 67(10) 66(100) 65(6) 53(7) 41(6) 39(6)

fragmented by losing either HNCS (**1a**, **b**) or CH_3OH (**3a**, **b**), depending on the heterocycle type. For **1**, $[M–C_5H_5]^+$ corresponds to protonated thiouracil. In the later stages of fragmentation, these ions lose either H or $OH^{\cdot}$ to form two radical cation species: $[M–C_5H_6]^{+\cdot}$ (6.4% TIC) corresponding to 2-thiouracil, and $C_4H_4N_2S^{+\cdot}$ (0.9% TIC) corresponding to 2-mercaptopyrimidine. These processes were not observed in the spectra of the thiazinopyrimidines **3a**, **b**, where the loss of CH_3OH is the only significant fragmentation route for $[M–C_5H_5]^+$. The loss of $OH^{\cdot}$ from $[M–C_5H_5]^+$ suggests that a proton is transferred to the carbonyl group in the course of the RDA fragmentation. No evidence could be obtained from the metastable spectra for the RDA fragmentation of **1** without H transfer (i.e., for the direct formation of $[M–C_5H_6]^{+\cdot}$ from the $M^{+\cdot}$ of **1**). Although the peaks of $[M–C_5H_6]^{+\cdot}$ are almost negligible (ca. 2% RA) for the norbornene-fused thiazinopyrimidines **3**, their metastable spectra suggest that the rather abundant $[M–C_6H_9O]^+$ (2.4-3.1% TIC) are not exclusively formed by the loss of CH_3OH from $[M–C_5H_5]^+$, but there is also a contribution from the RDA fragmentation (without H transfer) of $[M–MeO]^+$. Since $[M–MeO]^+$ is of low abundance in the spectra of **3** (0.5-0.6% TIC), the overall contribution of the RDA fragmentation via the loss of neutral cyclopentadiene (without H transfer) to the spectra of the norbornene-condensed compounds **1** and **3** under EI conditions is low and does not significantly depend on the type of the norbornene-fused heterocycle. This is in contrast with the previously reported thermal RDA decomposition of **1** upon melting, which furnished neutral thiouracil via cyclopentadiene elimination without H transfer [6].

Another important observation concerning the RDA fragmentations of thiazino-pyrimidine derivatives **3** and **4** is that carbocyclic RDA (i.e., cyclopentadiene elimination from $M^{+\cdot}$ as observed in the spectra of norbornene-fused **1** and **3**) and heterocyclic RDA (the elimination of $C_7H_9^{\cdot}$ from $M^{+\cdot}$ as observed in the spectra of norbornane-fused **4**) fragmentations are revealed as competitive processes in the spectra of **3**. The simultaneous occurrence of carbocyclic and heterocyclic RDA fragmentations under EI conditions has previ-

Table 2. Characteristic ions in EI spectra of **1–4** (ion abundances, $\%\Sigma_{25}$)

						Norbornene-fused			
Compound	$M^{+\cdot}$	$[M-C_5H_5]^+$ carbo RDA	$[M-C_5H_5-H]^{+\cdot}$	$C_5H_6^{+\cdot}$	$C_5H_5^+$	$[M-C_5H_5-HNCS]^+$ ($C_3H_4NO^+$)	$C_3H_3NO^{+\cdot}$	$C_7H_8^{+\cdot}$ hetero RDA	$C_7H_7^+$
1a	6.9	18.7[c]	6.4	22.4[c]	2.8	6.4[c]	3.7	—	1.1
1b	8.1	18.8[c]	6.4	22.5[c]	2.6	6.4[c]	3.8	—	0.9
3a	<0.1	26.8	0.5	15.8[c]	2.7	—	—	3.4[c]	9.2
3b	<0.1	29.3	0.6	16.0[c]	2.7	—	—	0.9[c]	5.5

						Norbornane-fused			
Compound	$M^{+\cdot}$	$[M-CO]^{+\cdot}$	$[M-C_7H_9]^+$ hetero RDA	$[M-C_5H_6]^{+\cdot}$ (**2a**,**b**)	$[M-C_5H_7]^+$ (**2a**,**b**)	$C_7H_{10}^{+\cdot}$	$C_7H_9^+$	$C_5H_7^+$	$C_5H_6^{+\cdot}$
2a	22.4	<0.1	—	9.7[c]	10.4	—	—	3.6[c]	2.6
2b	22.2	0.5	—	6.5[c]	13.4	—	—	3.2[c]	2.1
4a	9.0	6.8	14.0	1.6[a,c]	2.1[b]	1.6[c]	1.2	0.9[c]	22.8
4b	10.6	5.3	12.9	1.9[a,c]	2.8[b]	1.5[c]	1.5	1.1[c]	22.9

[a] $[M-CO-C_5H_6]^+$
[b] $[M-CO-C_5H_7]^+$
[c] corrected for isotopic contributions from the neighboring peak

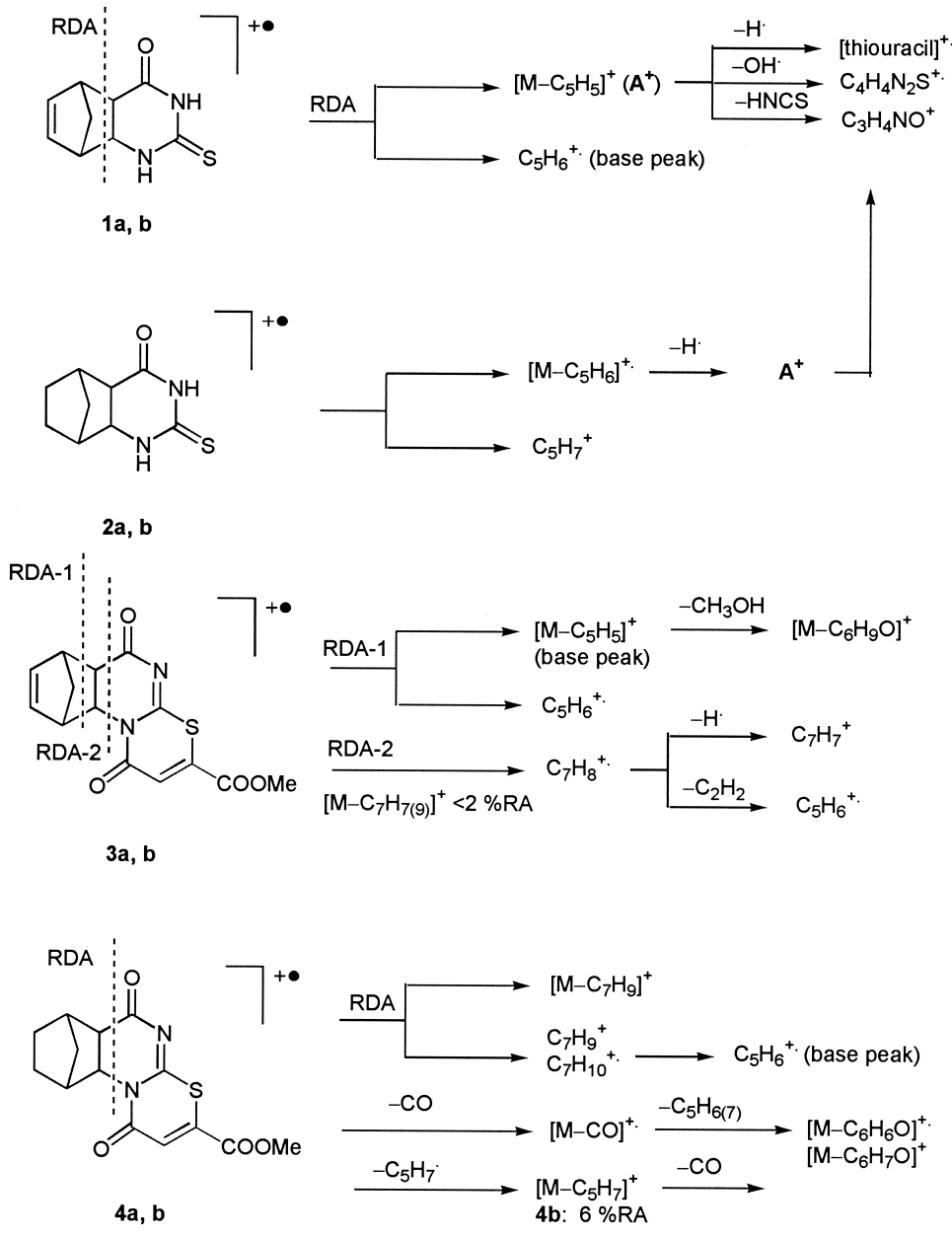

Scheme 2. Main fragmentation routes of compounds **1–4** under EI as established from metastable transitions and accurate mass measurements.

ously been reported for norbornene-condensed 1,3-oxazine derivatives [8]. For **3** and **4**, however, heterocyclic RDA fragmentation is important only for norbornane-condensed **4**, where there is no possibility for carbocyclic RDA. The relative abundance of $[M–C_7H_9]^+$ in the spectra of norbornene-condensed **3** is below 2% ($C_7H_8^{+\cdot}$ is also formed in this process), which means that the heterocyclic RDA fragmentation of $M^{+\cdot}$ is effectively suppressed by the carbocyclic RDA fragmentation.

Some other fragment ions observed in the EI spectra of **1–4** are listed in Table 2. The loss of CO from $M^{+\cdot}$, which is observed only for the norbornane-condensed heterocycles **2** and **4**, is much less important in the former case; ($[M–CO]^{+\cdot}$ contributes <0.5% to the TIC). $[M–CO–C_5H_{6(7)}]$ for **4a**, **b** is therefore listed in the same column as $[M–C_5H_{6(7)}]$ for **2a**, **b** in Table 2. Although a plausible mechanism for the rather abundant formation of $[M–C_5H_6]^{+\cdot}$ from norbornane-condensed thiouracils **2** is not obvious (it must involve at least two H transfers), the abundance of $C_5H_6^{+\cdot}$ in the spectra of **1–4** (Table 2) is lowest for **2** (2.1–2.6% TIC), which suggests that the mechanism of formation of $[M–C_5H_6]^{+\cdot}$ in this case (in the absence of RDA fragmentation) must be peculiar to compounds **2** only. It should be noted that $[M–C_5H_7]^+$ ions (which are directly formed from $M^{+\cdot}$) are observed in the spectra of all norbornane-condensed compounds **2** and **4**. For **2**, the composition of

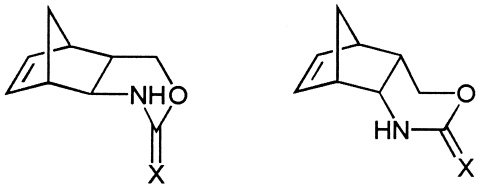

5a,b **6a,b**

Relative abundances ($\%\Sigma_{fragm}$) of $[MH-C_5H_6]^+$ in the CID spectra of MH^+ produced by CI (NH_3) [9]

	(a) X = O	(b) X = S
di*exo*-**5**	26.0	23.6
di*endo*-**6**	23.6	41.9

Scheme 3. Stereospecific RDA fragmentation of some norbornene-condensed heterocycles under CI conditions [9].

$[M–C_5H_7]^+$ is identical to that of $[M–C_5H_5]^+$ produced by RDA fragmentation of the norbornene-condensed **1** and corresponds to protonated thiouracil, $C_4H_5N_2OS^+$. It may be assumed that not only the compositions, but also the ion structures are identical for these species, as the metastable spectra demonstrate that the $[M–C_5H_7]^+$ formed from **2** further decomposes by losing either H or HNCS, similarly to the $[M–C_5H_5]^+$ originating from **1**. The main fragmentation routes of **1–4** are summarized in Scheme **2**. Fragmentation patterns involving various hydrocarbon losses dominate the spectra. Only a few significant peaks of ions related to heterocyclic cleavages (other than RDA) appear in the spectra; for instance, all the thiazinopyrimidine derivatives **3–4** produce abundant C_3HOS^+ (*m/z* 85, 2.4–3.1% TIC) due to the thiazine ring cleavage.

In general, the differences observed between the EI spectra of di*exo* and di*endo* isomers are in all cases insufficient for their reliable differentiation on the basis of the mass-spectrometric behavior of the isomers. In terms of the primary fragmentation processes, this means that the carbocyclic (as in **1**, **3**) and heterocyclic (as in **2**) RDA fragmentations of $M^{+\cdot}$, both of which involve H transfer, are practically non-stereospecific. Other fragmentations of $M^{+\cdot}$ (e.g., those resulting in the formation of $[M–C_5H_{6(7)}]$ in the cases of **2** and **4**) involve not only the transfer of one or two H atoms to the heterocyclic moiety, but also the consecutive cleavages of at least two C–C bonds. The stereochemical differences between the isomers would therefore already be lost after the initial C–C bond cleavage. Nevertheless, the abundances of the characteristic $[M–C_5H_{6(7)}]$ or $[M–CO–C_5H_{6(7)}]$ fragment ions are somewhat different for the stereoisomers comprising each pair of the norbornane-condensed compounds **2** and **4** (see Table 2).

CI Spectra

Compounds which undergo RDA fragmentation under EI conditions often, but not always, exhibit this type of fragmentation in their CI spectra too. For instance, the previously studied norbornene-condensed 1,3-oxazin-2(1H)-ones (and -thiones), which fragment by a (RDA + H) process under EI conditions to form $[M–C_5H_5]^+$ and $C_5H_6^{+\cdot}$, do not fragment at all under CI conditions with either isobutane or ammonia as reagent gas, but merely exhibit peaks of MH^+, $[M+NH_4]^+$, and M_2H^+ [9]. However, when the MH^+ produced by CI (ammonia) is subjected to collision activation, the CID spectra reveal moderately stereospecific RDA fragmentation to $[MH–C_5H_6]^+$, which is more abundant for the di*endo*-fused isomers of oxazinone derivatives and for the di*exo* isomers of oxazinethione derivatives (Scheme **3**) [9].

For **1–4**, the CI spectra obtained with either methane or isobutane as reagent gas demonstrated a substantial difference between the norbornane- and norbornene-condensed compounds. The former do not fragment at all under the CI conditions used, exhibiting only peaks of MH^+, $[M+X]^+$ (X = C_2H_5 or C_3H_5 for methane and $C_3H_{(3,5,7)}$ or C_4H_9 for isobutane), and M_2H^+. In contrast, the norbornene-condensed compounds **1** and **3** display prominent peaks of fragment ions because of the loss of C_5H_6 from MH^+ and $[M+X]^+$. In the methane CI spectra, the abundance of $[MH–C_5H_6]^+$ reaches 70% RA (base

Table 3. CI spectra of norbornene-fused stereoisomers **1** and **3**

	Isobutane CI				Methane CI			
Ion	di*exo*-**1a**	di*endo*-**1b**	di*exo*-**3a**	di*endo*-**3b**	di*exo*-**1a**	di*endo*-**1b**	di*exo*-**3a**	di*endo*-**3b**
M_2H^+	390 (6)	390 (6)	610 (1)	610 (2)	390 (3)	390 (4)	610 (2)	610 (4)
	389 (23)	389 (24)	609 (4)	609 (6)	389 (12)	389 (16)	609 (6)	609 (11)
$[M+C_3H_7]^+$	237 (5)	237 (4)	347 (1)	347 (1)	—	—	—	—
$[M+C_2H_5]^+$	—	—	—	—	223 (<1)	223 (<1)	333 (5)	333 (4)
MH^+	197 (7)	197 (7)	307 (9)	307 (9)	197 (5)	197 (5)	307 (9)	307 (9)
	196 (15)	196 (14)	306 (17)	306 (17)	196 (11)	196 (12)	306 (17)	306 (17)
	195 (100)	195 (100)	305 (100)	305 (100)	195 (100)	195 (100)	305 (100)	305 (100)
$[M+C_3H_7-C_5H_6]^+$	171 (6)	171 (6)	281 (4)	281 (4)	—	—	—	—
$[M+C_3H_5-C_5H_6]^+$	169 (4)	169 (4)	279 (3)	279 (3)	—	—	—	—
$[M+C_2H_5-C_5H_6]^+$	—	—	—	—	157 (26)	157 (26)	267 (23)	267 (23)
$[MH-C_5H_6]^+$	129 (7)	129 (7)	239 (17)	239 (13)	129 (18)	129 (17)	239 (70)	239 (55)

Table 4. Effects of sample partial pressure on rates of cluster ion formation and RDA fragmentation in the CI spectra of **3**

	Isobutane CI				Methane CI			
	M_2H^+, %RA		$[MH-C_5H_6]^+$, %RA		M_2H^+, %RA		$[MH-C_5H_6]^+$, %RA	
Entry[a]	di*exo*-**3a**	di*endo*-**3b**	di*exo*-**3a**	di*endo*-**3b**	di*exo*-**3a**	di*endo*-**3b**	di*exo*-**3a**	di*endo*-**3b**
1	2.0		14.8		6.1		70.4	
2	2.3		15.9		14.6		63.7	
3	3.7		16.8		25.2		53.4	
4		1.9		12.9		10.9		55.3
5		5.5		13.1		28.1		50.1
6		12.4		13.2		43.3		43.2
7		19.3		13.3		62.3		34.4
8		25.9		13.6				

[a] The insertion probe temperature was raised in 10°C steps during continuous scanning. Each entry represents an average of 10 consecutive scans recorded while raising the probe temperature from 150 to 190 °C (*i*-C_4H_{10} CI) and from 170 to 200 °C (CH_4 CI) for di*exo*-**3a** (entries 1–3); from 140 to 180 °C (*i*-C_4H_{10} CI) and from 150 to 180 °C (CH_4 CI) for di*endo*-**3b** (entries 4–8). The M_2H^+ abundances are indicative of the increasing sample pressure.

peak: MH^+), though it is 2–3 times lower in the isobutane CI spectra of **3a**. The relative abundances of the fragment and cluster ions (with respect to MH^+) vary, depending on the experimental conditions. Representative CI spectra of **1** and **3** are listed in Table 3.

The relative abundances of the cluster (M_2H^+) and fragment $(M+X-C_5H_6)^+$ ions were found to depend on the experimental conditions, and in particular on the sample partial pressure inside the CI ion source, which increased with heating of the direct insertion probe. Compounds **1**, which are more volatile, were introduced without heating of the probe. In the CI spectra of **3**, the relative abundance of M_2H^+ varied at different probe temperatures. It increased with rising temperature, apparently as a consequence of an increase in the sample partial pressure. It is seen from Table 4 that the abundances of $(M+X-C_5H_6)^+$ also vary with temperature, but on the average they are lower for the di*endo* isomers in each pair of compounds.

In contrast to the EI spectra, the RDA fragmentation of norbornene-condensed compounds under CI conditions, which proceeds without H transfer, was found to be slightly stereoselective, especially in the case of thiazinopyrimidine derivatives **3**. The rate of the RDA fragmentation of **3** under CI conditions is higher for the di*exo* isomers. It is seen from Table 4 that the relative abundance of $[MH-C_5H_6]^+$ in the methane CI spectra varies within the range 34–55% for **3b** and 53–70% for **3a**, depending on the experimental conditions. These ranges practically do not overlap, and the RDA fragmentation can therefore be classified as virtually stereoselective. In the isobutane spectra, however, the RDA fragmentation of MH^+ ions of **3a**, **b** is less stereoselective (13–14% vs 15–17%, see Table 4).

Although stereoselective RDA fragmentations are quite common in *cis*- and *trans*-cycloalkene-fused heterocycles [1, 4, 5], the case of compounds **3a**, **b** is noteworthy, as both the structures are *cis*-fused. Moreover, the difference in their fragmentation under CI is visible even without collision activation, unlike the spectra reported in [9].

In general, our results support the well-established hypothesis [1] that RDA fragmentations are more stereospecific when they occur without H transfer. For **1** and **3**, the RDA fragmentations initially lead to the even-electron heterocyclic cation under both EI and CI conditions, but the reaction mechanisms are different (the loss of $C_5H_5^{\cdot}$ under EI, and of C_5H_6 under CI conditions), which allows differentiation of the stereoisomers in the latter case because of moderately stereoselective fragmentation of MH^+.

Theoretical Considerations

Since the *cis*-fused heterocycles **3a** and **3b** are quite similar in structure, the moderate stereoselectivity of their RDA fragmentation observed under CI conditions merits a mechanistic study. The size of these molecules

Table 5. Calculated *vs.* experimental data on selected model compounds approximating the structures of norbornene-fused 2-thiouracil and its RDA fragmentation products

Compound	Parameter	AM1	PM3	6-31G*	Exp.
Cylopentadiene	ΔH_f, kcal/mol	+37.1	+31.8	—	33.2[a] (gas)
Norbornene	ΔH_f, kcal/mol	+26.0	+22.0	—	20.4[a] (gas)
	C(2)=C(3), Å	1.354	1.346	1.341[d]	1.336[b] (gas)
	C(5)−C(6), Å	1.542	1.546	1.561[d]	1.556[b] (gas)
5,6-dihydro-	ΔH_f, kcal/mol	−19.8	−15.8	—	—
2-thiouracil	C=O, Å	1.241	1.217	—	1.216[c] (solid)
	C=S, Å	1.610	1.639	—	1.676[c] (solid)

[a] Detected by calorimetry: W. R. Roth et al., *Chem. Ber.*, **1991,** *124*, 2499–2521.
[b] Electron diffraction: F. J. Chiang et al., *J. Mol. Struct.*, **1977,** *41*, 67–77.
[c] B. Kojic-Prodic et al., *Acta Crystallogr., Sect. B,* **1976,** *B32(4)*, 1099–1102.
[d] B. S. Jursic, *J. Mol. Struct. (THEOCHEM)* **1995,** *358*, 139–143.

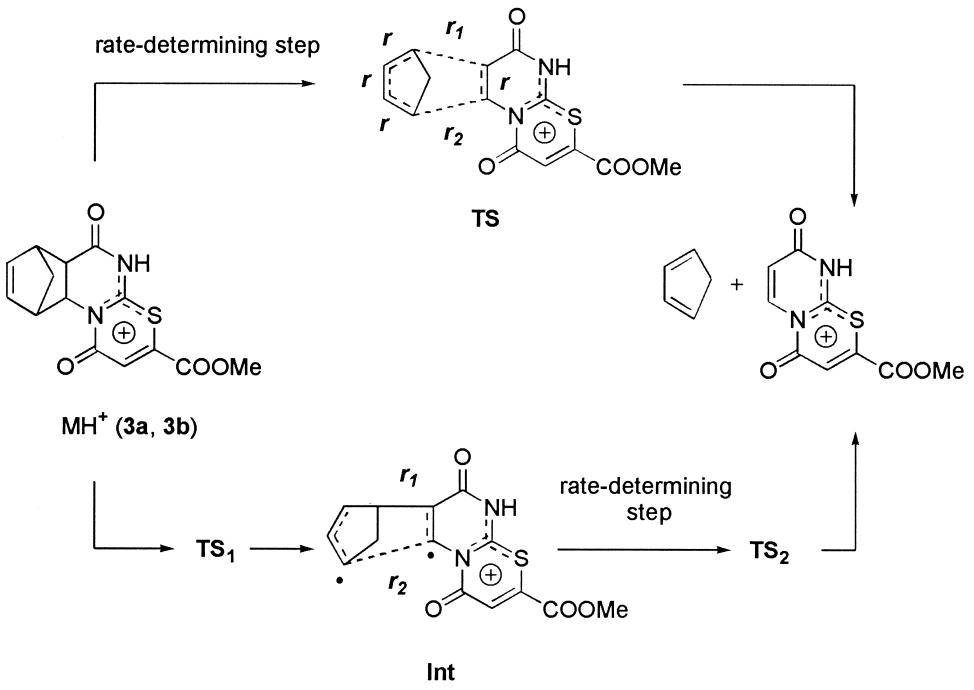

Scheme 4. Alternative reaction mechanisms for the RDA fragmentation of MH^+ (**3a**, **3b**) under CI conditions. See Tables 6 and 7 for the details.

renders the use of ab initio calculations impractical. At a lower level of theory, semiempirical methods have been used previously (in spite of their well-known limitations) in theoretical studies on various Diels-Alder (DA) and RDA reactions [10].

At present, the two most popular semiempirical procedures are the AM1 and PM3 methods [11], each with its own inherent weaknesses and strengths. Preliminary calculations performed on model compounds similar to **3** (Table 5) demonstrated that the PM3 method is superior to AM1 in reproducing their geometries, which may be crucial in determining the mechanism of RDA fragmentation.

Accordingly, PM3 calculations were performed using the MOPAC 6.0 program (Indiana University, IN) [12] to determine the geometries and enthalpies of formation of the transition states and possible intermediates for RDA fragmentations of MH^+ formed from **3a** and **3b** under CI. The HyperChem 5.01 program (Hypercube Inc., Gainesville, Florida, USA) was used as a graphical interface for drawing and vizualizing the structures and for preparing MOPAC input files. Only ground electronic states were considered. Complete geometric optimization was achieved using the EF (eigenvector following) routine and the PRECISE option by reducing RMS gradients to 0.001 kcal/mol/Å. Transition state structures were located by the SADDLE routine using optimized geometries of the reactants and products as input without any specific assumptions or restrictions concerning the saddle point geometry. The saddle points returned by the SADDLE routine were optimized using either the TS or NLLSQ routines to obtain transition-state structures which were then characterized by force calculations (FORCE routine) to verify that they had one, and only one, negative force constant (imaginary frequency).

An analysis of the MH^+ structures that could possibly be formed from **3** under CI conditions showed that the protonation of the sp^2-hybridized nitrogen produces the most stable species (Scheme **4**). Its enthalpy of formation is, for example, lower by 23 kcal/mol than

Table 6. Parameters of the RDA fragmentation of MH^+ (**3a**, **3b**) via concerted synchronous mechanism (for the notation, cf. Scheme **4**) calculated by the PM3 method using the closed-shell restricted Hartree-Fock (RHF) approximation with and without configuration interaction (C.I.)

Method	MH^+ isomer	ΔH_f(MH), kcal/mol	ΔH_f(TS), kcal/mol	E_a, kcal/mol	TS geometry			
					r, Å	r_1, Å	r_2, Å	α[a]
RHF	di*exo*	100.3	146.3	46.0	1.406–1.408	2.180	2.165	0.003
	di*endo*	99.9	144.9	45.0	1.406–1.407	2.161	2.161	0.000
RHF/C.I.	di*exo*	100.3	146.2	45.9	1.405–1.409	2.159	2.188	0.007
	di*endo*	99.9	144.8	44.9	1.405–1.408	2.147	2.178	0.007

[a] Degree of asynchromicity, $\alpha = |r_1 - r_2|/(r_1 + r_2)$.

Table 7. Parameters of the RDA fragmentation of MH^+ (**3a**, **3b**) by a stepwise mechanism *via* biradical intermediates (for the notation, cf. Scheme **4**) calculated by the PM3/UHF method

MH^+ isomer	$\Delta H_f(MH^+)$, kcal/mol	TS_1			Int		TS_2		E_a, kcal/mol
		ΔH_f	r_1, Å	r_2, Å	ΔH_f	r_1, Å	ΔH_f	r_1, Å	
di*exo*-	100.3	127.4	1.56	2.26	113.4	1.54	132.0	2.08	31.7
di*endo*-	99.9	127.2	1.56	2.26	112.3	1.54	130.9	2.08	31.0

that of MH^+ produced by the protonation of the ester group.

Calculations using the closed-shell restricted Hartree-Fock (RHF) method located highly symmetrical transition states (TS, Scheme **4**) corresponding to concerted RDA fragmentations of MH^+ in both **3a** and **3b** (Table 6). The inclusion of configuration interaction involving HOMO and LUMO (RHF/C.I. in Table 6; MOPAC keyword C.I. = 2) resulted in less symmetrical TS structures but did not significantly change their enthalpies of formation. It is seen from Table 6 that the calculated activation energies for the concerted RDA fragmentations of the di*exo*- and di*endo*-fused MH^+ structures only differ by ca. 1 kcal/mol, a value which is below the estimated error of semiempirical calculations [13, 14].

Both the open-shell RHF and unrestricted Hartree-Fock (UHF) methods converged to highly asymmetrical transition states TS_2 corresponding to stepwise RDA fragmentations via biradical intermediates **Int** (Scheme **4**). The energy barriers (Table 7) for the stepwise RDA fragmentations are lower than for the concerted reaction path, but the di*exo*/di*endo* difference is again less than 1 kcal/mol.

RDA fragmentations in di*exo*/di*endo*-fused isomers can proceed stereoselectively even via the stepwise mechanism, but only if the formation of TS_1 is the rate-determining step, i.e., $\Delta H_f(TS_1) > \Delta H_f(TS_2)$, because the di*exo*/di*endo* stereochemical difference between the two isomers is lost after the first C–C bond is broken. Stereochemically speaking, the two intermediates **Int** formed from MH^+ of **3a** and **3b** are still optical antipodes, but the system is no longer rigid, and free rotation around the remaining single C–C bond may occur prior to the formation of TS_2. Since the calculated ΔH_f values show the formation of TS_2 to be the rate-determining step (Scheme **4**), the observed moderate stereoselectivity of the RDA fragmentation is probably due to a competition between the two fragmentation mechanisms. Some of the MH^+ ions would undergo stereoselective fragmentation via the concerted route, whereas the majority of them would decompose nonselectively via the stepwise mechanism, which has the lower energy barrier. On the macroscopic scale, this would result in a moderately stereoselective fragmentation.

It is seen from Tables 6 and 7 that the PM3 calculations did not provide definite explanations in terms of energy for the experimentally observed differences in the fragmentation rates of di*exo*- and di*endo*-fused MH^+ of **3**. A similarly small difference between the energy barriers was previously observed [15] in the thermal RDA decomposition of di*exo*- and di*endo*- norbornene-fused 2-aryl-1,3-oxazinones at 388-398 K, where the experimentally determined rate constants differed considerably (Scheme **5**), but the activation energies for the decomposition of the di*exo*- and di*endo*-isomers (calculated using the Arrhenius formula) differed by less than 1 kcal/mol.

There are, however, some structural differences between the symmetrical transition states for the MH^+ of **3a** and **3b** (Table 6). The differences are probably too subtle to be reflected in the respective enthalpies of formation, but they could provide at least a tentative explanation for the slightly faster RDA fragmentation in the case of the di*exo*-fused isomer. Of the two TS structures (Scheme **6**), the one corresponding to the fragmentation of the di*exo* isomer is sterically more crowded. The C2–C4 and C3–C5 distances (Scheme **6**) are shorter by ca. 0.05 Å (2.69 Å vs 2.74 Å in the di*endo* structure). There are also close C–H contacts between C2 and H4 (2.58 Å), and between C3 and H5 (2.55 Å), which are absent in the di*endo* structure. Conversely, the C–H distances between these hydrogens and the methylene carbon in the di*endo* structure are considerably greater (2.74–2.75 Å). This steric repulsion may be the underlying cause for the r_1 and r_2 distances (e.g., C1–C4 in Scheme **6**) between the reaction centers being longer by 0.01–0.02 Å in the TS corresponding to the di*exo*-fused isomer. Apparently, the change in the calculated TS energies caused by these geometry differ-

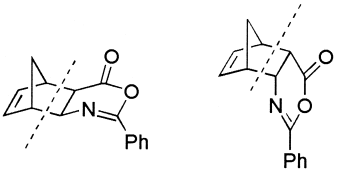

	di*exo*	di*endo*	
RDA rate constants,	2.25	4.99	388 K
$k \times 10^5\ s^{-1}$	6.15	13.40	398 K
E_a, kcal/mol	30.9	30.5	

Scheme 5. Experimentally-determined parameters of the thermal RDA decomposition of di*exo*- and di*endo*- norbornene-fused oxazinones at 388-398 K [15].

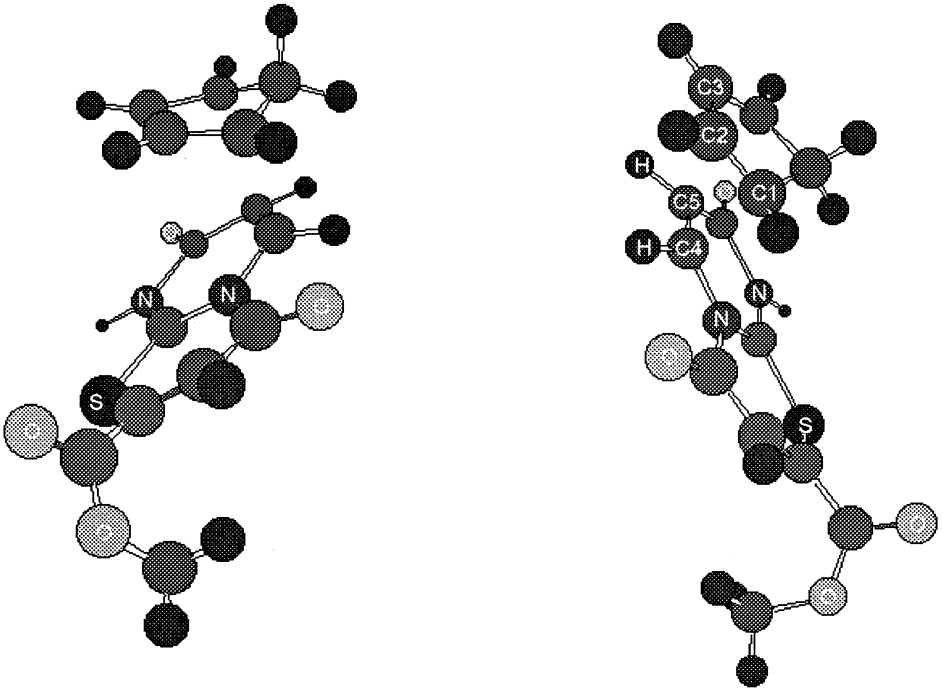

Scheme 6. Transition states (**TS**, Table 6) for the concerted retro-Diels-Alder fragmentation of di*endo* (left) and di*exo* (right) fused isomers of MH^+ (**3a**, **3b**) as calculated by the PM3/RHF method. The C—C bonds being broken are not shown for clarity.

ences is below the accuracy of the computational method used.

Conclusion

The EI mass spectra of di*exo*- and di*endo*-fused isomers of norbornane/ene-condensed 2-thiouracil and 1,3-thiazino[3,2-*a*]pyrimidine derivatives exhibit only minor differences, but they provide valuable information on the concurrent RDA fragmentations (carbocyclic and heterocyclic) involving the norbornene and thiazinopyrimidine substructures. The carbocyclic RDA fragmentation (the splitting off of neutral cyclopentadiene molecule) has lower activation energy and occurs under CI conditions as well. The experimentally observed moderate stereoselectivity of this RDA fragmentation in compounds **3a** and **3b** under CI conditions is remarkable, as the heterocycles in both isomers are *cis*-fused to norbornene.

Acknowledgments

The authors are indebted to OTKA (Grant T25415), CIMO (Centre for International Mobility) and the Academy of Finland (Grant no. 4284) for financial support.

References

1. Mandelbaum, A. In *Applications of Mass Spectrometry to Organic Stereochemistry*; Splitter, J. S.; Tureček, F., Eds.; VCH: New York, 1994; p 299–324.
2. (a) Miketova, P.; Schram K. H.; Whitney J. L.; Kerns E. H.; Valcic S. *J. Nat. Prod.* **1998** *61(4)*, 461–467; (b) Font, E.; Lasanta, S.; Rosario, O.; Rodriguez, J. F. *Nucleosides, Nucleotides, and Nucleic Acids* **1998** *17(5)*, 845–853; (c) Rohr, G. E.; Riggio, G.; Meier, B.; Sticher, O. *Phytochem. Anal.* **2000,** *11(2)*, 113–120.
3. Denekamp, C.; Weisz, A.; Mandelbaum, A. *J. Mass Spectrom.*, **1996,** *31*, 1028–1032.
4. Pihlaja, K.; Ovcharenko, V. V.; Stajer, G. *J. Am. Soc. Mass Spectrom.* **1999,** *10(5)*, 393–401.
5. Lemaire, D.; Serani, L.; Laprevote, O.; Ovcharenko, V. V.; Pihlaja, K.; Stájer, G. *Eur. Mass Spectrom.* **1999,** *5(4)*, 253–257.
6. (a) Sohár, P.; Szoke-Molnar, Z.; Stájer, G.; Bernáth, G. *Magn. Reson. Chem.* **1989,** *27*, 959–963; (b) Himottu, M.; Pihlaja, K.; Stájer, G.; Bernáth, G.; Vainiotalo, P. *Org. Mass Spectrom.* **1991,** *26*, 493–497.
7. Stájer, G.; Szabó, A. E.; Sohár, P. *Heterocycles* **1999,** *51(8)*, 1849–1854.
8. Pihlaja, K.; Himottu, M.; Ovcharenko, V. V.; Frimpong-Manso, S.; Stájer, G. *Rapid Commun. Mass Spectrom.* **1997,** *11(3)*, 249–252.
9. Partanen, T.; Vainiotalo, P.; Stájer, G.; Bernáth, G.; Pihlaja, K. *Org. Mass Spectrom.* **1990,** *25*, 615–619.
10. Dewar, M. J. S.; Jie, C. *Acc. Chem. Res.* **1992,** *25*, 537–543.
11. (a) Dewar, M. J. S.; Zoebisch, E. G.; Healy, E. F.; Stewart, J. J .P. *J. Am. Chem. Soc.* **1985,** *107*, 3902–3909; (b) Stewart, J. J .P. *J. Comp. Chem.* **1989,** *10*, 209–221.
12. Stewart, J. J. P. *MOPAC 6.0, QCPE No. 455*; Indiana University, Bloomington, Indiana.
13. Levine I. N. *Quantum Chemistry, 4th ed.*; Prentice Hall: New Jersey, 1991; pp 597–599.
14. Anh, N. T.; Frison, G.; Solladié-Cavallo, A.; Metzner, P. *Tetrahedron* **1998,** *54*, 12841–12852.
15. Stájer, G.; Mód, L.; Szabó, A. E.; Fülöp, F.; Bernáth, G. *Tetrahedron* **1984,** *40*, 2385–2393.